Three-State 2′,7′-Difluorofluorescein Excited-State Proton Transfer Reactions in Moderately Acidic and Very Acidic Media

Angel Orte,[†] Eva M. Talavera,[†] António L. Maçanita,[‡,§] Juan Carlos Orte,[†] and Jose M. Alvarez-Pez*[,†]

Department of Physical Chemistry, University of Granada, Cartuja Campus, 18071 Granada, Spain, Centro de Química Estrutural, Departamento de Engenharia Química, Instituto Superior Técnico, Av.[a] Rovisco Pais s/n, 1049-001, Portugal, and Instituto de Tecnologia Química e Biológica, Oeiras, Portugal

Received: March 11, 2005; In Final Form: August 3, 2005

2′,7′-Difluorofluorescein (Oregon Green 488, OG488) is a novel fluorescein dye derivative which presents important advantages for improving the fluorimetric applications in the biomedical and biochemical sciences. In aqueous solution it displays four prototropic forms, namely cation (C), neutral (N), monoanion (M), and dianion (D). In previous works, we found (*J. Phys. Chem. A* **2005**, *109*, 734−747, 2840−2846) that OG488 undergoes excited-state proton transfer reactions, which may affect the results from applications using this dye. We established that the excited-state proton transfer (ESPT) reactions between neutral, monoanionic, and dianionic forms of OG488 are promoted by acetate buffer, and we characterized the ground and excited species involved. We also solved the kinetics of the prototropic reactions using global compartmental analysis. In the present paper, we extend our study on the ESPT reactions of OG488 to acidic media, in which only the three prototropic species cation, neutral, and monoanion coexist. We have solved the kinetics of the three-state ESPT reaction by means of global three-compartmental analysis of a fluorescence decay surface in moderately acidic media (pH between 1.1 and 3.0), recovering the kinetic and spectral parameters of this three-state system. This system is one of the most complex solved to date, due to the strong overlap of the absorption and emission spectra of the neutral and monoanionic forms of OG488. We also found that the cation behaves as "super" photoacid, showing a very high deprotonation rate constant (1.04×10^{11} s^{-1}) and an enhanced acidity. Therefore, we also carried out experiments at very high perchloric acid concentrations, dealing with some other effects which become noteworthy at these [H^+]. The presence of xanthylium cation quenching due to "free" water molecules, and the reduction in the amount of water clusters acting as proton acceptors, are processes which alter notably the time course of the excited-species in this high [H^+] range.

Introduction

The fluorescein-based dye 2′,7′-difluorofluorescein (Oregon Green 488, OG488) is widely used in several fields of science, such as biochemistry, biomedicine, neurosciences, etc.[1] This fluorescence probe has recently been synthesized,[2] and its rapid popularization encouraged us to carry out an in-depth study on its fundamental spectroscopic and acid−base features. Since fluorination does not affect acid−base groups, Oregon Green 488 (OG488), as fluorescein, displays four prototropic forms in aqueous solutions: cation (C), neutral (N), monoanion (M), and dianion (D), of which the dianionic form shows much higher fluorescence than the others. Two fluorine atoms impart higher polarity to the molecule, lessening pK_a values, as occurs in chlorinated fluoresceins.[3] This is favorable in biochemical applications, since, at biological pH, the prevalent prototropic form is the dianion. In a previous work we provided a comprehensive description of the ground-state acid base equilibria of the four prototropic forms of OG488 and their ground-state pK_a values, as well as the steady-state fluorescence emission behavior of each species.[4]

The excited-state proton transfer (ESPT) reactions of fluorescein[5,6] are important because they must be taken into account for a correct interpretation of the fluorescence emission data when the dye is used as a fluorescent probe. Therefore, we decided to investigate this sort of reaction in OG488. In our previous papers on OG488, we described the excited-state proton exchange reactions in aqueous solution at pH values at which the neutral, monoanion, and dianion species are involved. Some of these reactions are spontaneous and others need a suitable proton acceptor/donor present at sufficiently high concentration. We solved the excited-state kinetics of these reactions by means of global compartmental analysis (GCA) of a fluorescence emission decay surface,[4] and we correlated the kinetic and associated spectral parameters recovered with steady-state emission spectra.[7] GCA is a powerful tool for unraveling the rate constants and relevant spectral parameters, in a single step analysis,[8] and it has been frequently used in the study of ESPT reactions, both in the absence[9] and the presence[4,6] of a suitable proton acceptor/donor.

In this work, we complete the study of the OG488 excited-state reactions in aqueous solution dealing with the acid range of the pH scale from 1.1 to 3.0 by using perchloric acid for changing acidity. We chose this acid because negligible quenching is induced by perchlorates at high concentrations, whereas chloride anions produce strong quenching on the OG488 cation fluorescence emission. The cationic, neutral, and monoanionic species are involved in this pH range. The dianion can be ignored since it is not present in the ground-state at the pH

* Corresponding author. E-mail address: jalvarez@ugr.es.
[†] University of Granada.
[‡] Instituto Superior Técnico
[§] Instituto de Tecnologia Química e Biológica.

10.1021/jp051264g CCC: $30.25
Published on Web 09/14/2005

values used in this work, and its formation in the excited-state requires the presence of a suitable proton acceptor/donor.[4] Furthermore, the quinoid form of OG488 was the only neutral tautomer considered, since the lactonic form is neither absorbing nor emitting in the visible range, and the low amount of zwitterions seems to convert into quinoid in the excited-state,[4] and can thus be ignored, as occurs in fluorescein.[10] We have established a three-state excited-state kinetic scheme, based on the coexistence of three prototropic forms and the characteristics of fluorescence decays. This has been solved by using a three-compartment GCA. Among the few three-compartmental systems solved,[11,12] the present system is one of the most complex due to the large spectral overlap of the species involved. In addition, few ESPT kinetics including more than two excited species have been successfully investigated. Seixas de Melo et al. published[13] a general method for solving the "kinetic triangle", a three-state excited-state scheme with each species being formed from the other two species, and applied it to 7-hydroxy-4-methylcoumarin[13] and harmine.[14] Other examples of three-state excited-state reactions can be found for other dyes such as norharmane,[15] chromotropic acid,[16] and riboflavin.[17]

It is well-known that excitation causes a reduction in the pK_a^* value of the prototropic equilibrium between cationic and neutral forms of fluorescein and its derivatives.[18,19] In our previous paper, we emphasized that the OG488 cation emission was not detected at acid concentration below 2 M, although its absorption was clearly observed at this [$HClO_4$].[4] So the cationic form of OG488 in aqueous solution can be considered as a cationic photoacid, a kind of photoacid that, after excitation, undergoes a fast isoelectric proton-transfer reaction which does not involve the generation of an ion-pair. In general, these cations are stronger photoacids than the so-called neutral photoacids (aromatic alcohols like naphthol, pyrenol, and derivatives) which dissociate, generating an ion-pair.[20]

The spectral characteristics of the aqueous solutions of OG488 agree with the general consideration about the acidic character of excited aromatic alcohols.[21] It is also in accordance with the idea that the presence of the positive charge in the carbon 9 of the protonated xanthene ring provides an additional driving force for deprotonation of the hydroxyl group, enhancing the photoacid character, as was described by Bardez et al. for the cations of bifunctional hydroxyquinolines, a family of stronger photoacids than the corresponding monofunctional compounds, naphthols, or methoxyquinolines.[22] So, the OG488 cation can behave as an enhanced photoacid,[23] dissociating via an isocharged process such as 1-aminopyrene[24] or 6-hydroxyquinoline.[22] The fact that the OG488 cation is such a strong photoacid means that high acid concentrations are required for detecting the cation emission.[4] Therefore, in this work, we have also studied the [H^+] range between 11.1 M and pH below 1.0, also using perchloric acid for changing acidity.

At these high acid concentrations, there are some other effects that can drastically influence the rate of the ESPT reactions, such as viscosity changes, which alter the diffusion-controlled processes,[25] or the decreased availability of water molecules to accept a proton, which is reduced at high electrolyte concentrations, when the fraction of water molecules involved in hydration process reduces the free water amount behaving as proton acceptor. The nature of the proton acceptor in deprotonation to water has been widely studied,[26] and it is important in cases of a reduced amount of "free water", such as water:alcohol mixtures and highly concentrated acid solutions. There have been several proposals regarding the effective proton acceptor in excited-state deprotonation of photoacids. Most of the studies suggested a four-molecule water cluster (4 ± 1) as the critical size of the acceptor for the deprotonation of aromatic alcohols in varied solvents.[27] Smaller cluster size has also been proposed as proton acceptors in strong neutral photoacids, such as cyanonaphthols,[28] 4-hydroxy-1-naphthalenesulfonate,[29] HPTS (8-hydroxy-1,3,6-trisulfonatepyrene),[30] or hydroxyalkylnaphthols,[31] the argument being that the apparent size of the water cluster acceptor decreases with the higher strength of the photoacid.[29] Therefore, the cluster size seems to depend on the photoacid employed and the suitable orientation of the water cluster is also important.[32] Although neutral and cationic photoacids cannot be compared to each other in reference to their dissociation reaction, and some authors reported that the model of water clusters as proton acceptors was not applicable to cationic photoacids,[24] this model has been used in other cationic photoacids such as hydroxyquinolines.[22] According to Pines and Fleming proton transfer from cationic photoacids to the solvent is governed by proton solvation. These photoacids should therefore be good probes to test the proton solvation complex, isolating it from the other solvation processes which accompany neutral photoacid dissociation.[24] Modern theories of proton solvation in water propose a water dimer as the most important proton acceptor in concentrated acid solutions. On the other hand, ab initio simulations of proton transfer in water indicate that $H_5O_2^+$ cation is almost isoenergetic with $H_9O_4^+$ cation. Some of these calculations further indicate that proton transfer reactions from cationic photoacids only require solvent ability to stabilize the ejected proton along the proton-transfer coordinate, by way of appropriate solvation structures. These structures are specific for each photoacid.[20]

Another important issue in the photoacids reactivity is the influence of diffusion, leading to nonexponential decays subject to the Smoluchowski theory[33] generalized by Debye.[34] In the photoacids chemistry, the rapid reassociation of the ejected proton, the so-called geminate recombination, is caused by the mechanistic influence of diffusion. This was originally observed by Pines and Huppert[35] and further analyzed theoretically and experimentally.[36−39] In general, all these processes induce nonexponential decay traces, due to the time dependence of the rate constants (transient effect), although the conventional approximation of time-independent rate constants and multiexponential decays has been widely used providing excellent results.[40] The proper detection of the transient stage and the power law limit has frequently involved their study in high viscosity solvents in order to decrease the diffusion of the reactants,[30,41,42] or the use of approximations such as the convolution kinetics approach[43,44] (developed by Agmon and Szabo[45]), which has been found to predict with high accuracy the initial and intermediate times of a diffusion-influenced transient kinetics. Modern interpretations of the influence of diffusion in proton transfers have required higher time resolution. Femtosecond experiments have thus shed light on the determination of intrinsic rate constants and provided insights into the processes taking place in acid−base reactions,[39,46] although these studies should deal with other issues such as solvation dynamics.

As cited before, we shall deal in the present work with concentrated acid solutions, in which the available "free" water amount and the water structure can be drastically altered, influencing the deprotonation rates. Apart from this effect, water appears to specifically affect the fluorescence lifetimes of some dyes. For instance, Bardez et al. described a quenching process due to water of the neutral (protonated) chromotropic acid at high perchloric concentrations,[16] and Joshi et al. found that

salicylic acid also shows quenching due to water.[47] Moreover, the parent compounds of fluorescein cations, the 9-xanthylium cations, are quenched by water molecules, as indicated by the decrease in fluorescence lifetimes with decreasing acidity.[48,49] For a series of 9-xanthylium cations values between 1.86×10^6 and 2.51×10^9 M^{-1} s^{-1} were obtained for the quenching rate constant.[49] One possible explanation for this water quenching is the enhanced nonradiative deactivation processes due to water. The existence of differential nonradiative decay processes depending on water content in alcohol:water mixtures has been frequently noticed in a number of compounds, as aminonaphthalenes, aminonaphthalenesulfonates,[50] aminonaphthalimide derivatives,[51] or 5-cyano-2-naphthol.[41]

In brief, this work completes the study of the kinetic and associated spectral parameters from the ESPT reactions of the novel dye OG488, namely, the reactions between cation, neutral, and monoanion, at pH values between 1.1 and 3, by means of three-compartmental GCA. In addition, we also studied the cation/neutral reactions at highly concentrated acid solutions, which reveal different processes related to the decrease in the amount of "free" water with increasing acidity.

Materials and Methods

Reagents and Solutions. 2′,7′-Difluorofluorescein (OG488) was obtained from Molecular Probes Inc. and used without further purification. Perchloric acid (Merck, analysis grade, 70−72%) and sodium hydroxide (from Panreac) were used for changing acidity. Sodium perchlorate from Panreac was used to fix ionic strength. A slight quenching of the OG488 fluorescence was found in the presence of perchlorate ions. Stock solutions of 2′,7′-difluorofluorescein (10^{-4} M) in 1.27×10^{-3} M NaOH were prepared using Milli-Q water. The required volumes of the OG488, perchloric acid, sodium perchlorate, and sodium hydroxide stock solutions were used to obtain the desired concentrations of OG488, pH, and ionic strength. OG488 solutions were kept cool in the dark when not in use to avoid possible deterioration by exposure to light and heat, as occurs in fluorescein.[52]

Absorption and Steady-State Fluorescence Measurements. Absorption spectra were recorded by means of a GBC Cintra 10e UV−vis spectrophotometer, equipped with a temperature-controlled cell holder, using 10 × 10 mm cuvettes. The blank solution was a perchloric acid solution of the same concentration as the sample. The steady-state fluorescence spectra were acquired on a Perkin-Elmer LS 55 spectrofluorometer, using 10 × 10 mm cuvettes, and corrected through internal files provided with the instrument. A temperature-controlled cell holder is also available in the spectrofluorometer. All measurements were performed at room temperature (20 °C).

Instrument for Time-Resolved Fluorescence Measurements. The time-correlated single-photon counting technique was used to record the fluorescence decay traces of OG488 solutions using two instrumental setups. A complete fluorescence decay surface was recorded on a home-built laser-based time-resolved fluorescence instrument. This system employs a regenerative mode-locked Ti:sapphire laser, pumped by an argon ion laser. A pulse selector, a flexible harmonic generator, a synchronously pumped optical parametric oscillator, a Berek compensator, and a Glan-Thomson polarizer complete the excitation path. This setup allows fast and easy tuning of excitation wavelengths over a range of 240 to 1300 nm and provides stable 1−2 ps pulse trains. A beam splitter separates 5% of the excitation light for generating the STOP signal in a high-speed photodiode. Fluorescence was collected at 90° geometry after a collimating lens and a sheet polarizer (set at the magic angle with respect to the excitation polarization) and detected using a cooled microchannel plate (MCP) photomultiplier, after a double subtractive monochromator. The signal from the MCP is amplified and delayed, being the START signal in a MCS card installed on a computer equipped with the software SPC 630, providing the constant fraction discriminator and the time-to-amplitude converter (TAC). Full details of the picosecond laser system have been reported elsewhere.[53] 10 × 10 mm cuvettes were used to acquire the fluorescence decay traces. Instrument response profiles were recorded using a light scatterer, LUDOX colloidal silica solution (fwhm of 28 ps, see Figure 9 for a representation of the instrument profile). Histograms of the sample decay traces and instrument profiles were recorded until 10^4 counts were reached at the peak channel, and using two scales, 5.94 and 1.22 ps/channel, along 4096 channels. The complete fluorescence decay surface was composed of traces acquired at the excitation wavelength of 420 nm (this excites three species: cation, neutral, and monoanion), the emission wavelengths of 450 (only cation emits), 470, 510, 515, 550, and 580 nm, and different perchloric acid concentrations between 11.1 M, and a pH value of 2.98.

For acquiring the decay traces of OG488 solutions at different temperatures, a commercial Edinburgh Analytical Instrument FL900 ns time-resolved spectrofluorometer operating in the time-correlated single photon counting mode was used. The excitation source is a free running discharge flash lamp (nF900 Nanosecond Flashlamp) operating at 7.0 kV, 0.40 bar (H_2), and a frequency of 40 kHz, with a temperature-controlled cell holder. The decay traces were collected, using 10 × 10 mm cuvettes,

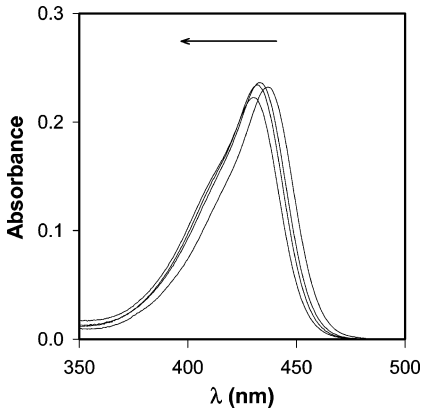

Figure 1. Absorption spectra of 5.0×10^{-6} M OG488 aqueous solutions at perchloric acid concentrations of 10.5, 8.2, 7.0, and 2.3 M. The arrow indicates the increase in acid concentration.

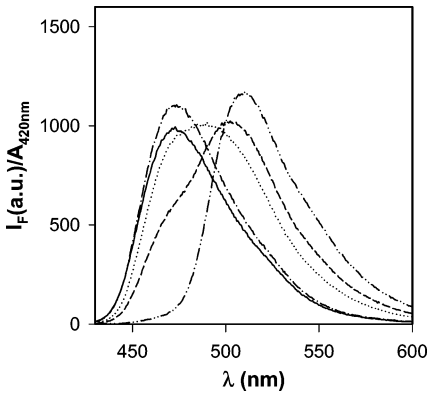

Figure 2. Steady-state emission spectra ($\lambda^{ex} = 420$ nm), normalized by the absorbance, of 5.0×10^{-6} M OG488 aqueous solutions at $[HClO_4] = 2.3$ (•• −), 4.7 (− −), 5.9 (•••), 9.4 (• −), and 10.5 M (−).

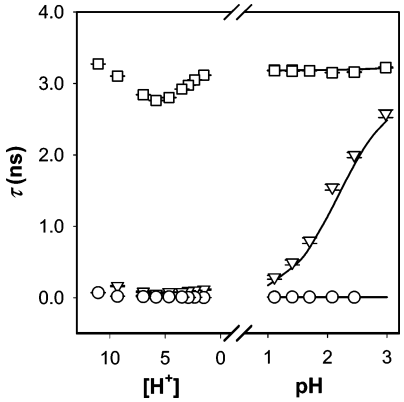

Figure 3. Fluorescence decay times recovered from global analyses (symbols) of decay traces from OG488 aqueous solutions at pH values between 0.3 and 3.0 (right), and perchloric acid concentrations between 1.5 and 11.1 M (left). Lines were calculated using the GCA equations (see Supporting Information), through the eigenvalues of the compartmental matrix **A** with the rate constant values of Table 1.

along 1024 channels of the multichannel analyzer with a time-per-channel of 48 ps/channel, until the typical value of 10^4 counts at the maximum was reached. The instrument response function was obtained using a light scattering solution (LUDOX colloidal silica, Sigma). We recorded fluorescence decay traces of an OG488 solution at $[HClO_4] = 9.4$ M, at the temperatures of 278, 293, and 318 K, using $\lambda^{ex} = 420$ nm and two different λ^{em}: 450 and 515 nm.

The decay traces of solutions at the same acid concentration and temperature were globally analyzed by means of the usual deconvolution methods, based on Marquardt's minimization. The tested decay functions were multiexponentials, where the decay times were linked as shared parameters, whereas the preexponential factors were local adjustable parameters.

Results

Absorption Measurements of OG488 Aqueous Solutions at pH Values below 3. In our previous paper, a comprehensive study of absorption and ground-state equilibria of OG488 was carried out. Scheme 1 shows the different species and pK_a values found in aqueous solutions at the -0.1 to $+12.4$ pH range studied.[4] In the present paper, we focus on the behavior of OG488 at pH values below 3. According to our previous work, only cation, neutral, and monoanion exist below pH 3. The absorption spectra of the solutions used in the present work, in the pH range 1.1−3.0, are in complete agreement with the expected spectra based on the reported pK_a and molar extinction coefficients (ϵ_i). This confirms the reliability of the pK_a and ϵ_i values previously recovered.

Additional features were noticed at very high acid concentrations. Thus, when $HClO_4$ concentrations above 2 M were used, the single absorption band with maximum molar extinction coefficient at 437.5 nm, recovered for the OG488 cation[4] showed a gradual blue shift with increasing acid concentration, from 437.5 nm (at $[HClO_4] = 2.3$ M) to 430 nm (at $[HClO_4] = 11.1$ M), (Figure 1). The spectra showed no apparent modification in shape and no isosbestic points were found. Instead, the shift is continuous with increasing perchloric acid concentration.

Steady-State Fluorescence Measurements of OG488 Aqueous Solutions at pH below 3. The most remarkable feature of the steady-state fluorescence spectra of OG488 below pH 3 is that the cation emission is not detected at acid concentrations below 2 M (Figure 2), although cation absorption is clearly observed in the range between pH 2 to 2 M $HClO_4$ (Figure 1). Higher acid concentrations are needed to detect the cation fluorescence emission. This effect was described in our previous paper[4] and attributed to the rapid deprotonation of the excited C, since it becomes a strong photoacid. The shape of the emission spectrum remained unchanged in the pH range between 0 and 2.12, showing a maximum at 513 nm, and a shoulder around 550 nm. Since $pK_C = 1.02$, and $pK_N = 3.61$,[4] the mole fraction of the ground-state C in this pH range (0−2.12) has values between 0.91 and 0.07, whereas the mole fraction of the N species changes between 0.09 and 0.90. The main excited form is thus C with decreasing pH, which is confirmed by observation of the excitation spectra. When acid concentration was increased above 2 M, a new emission band with a maximum at 471 nm appeared, and the emission band of N disappeared. This new band was assigned to the cation emission, as in fluorescein.[18,19] Therefore, the emission of C is detected only at extreme acidic conditions, indicating its rapid deprotonation in the excited-state. Figure 2 shows emission spectra of OG488 aqueous solutions at perchloric acid concentrations between 2.3 and 10.5 M. At acid concentrations above 8.2 M the emission spectral shape remained unchanged, as derived from observation of the normalized spectra (not shown), although a slight decrease in the emission intensity was detected with increasing acid concentration. Nevertheless, at perchloric acid concentration of 11.1 M, the excitation at the red edge of the absorption band results in a red-shift in the wavelength of the emission maximum, although with no change in the spectral shape. Thus, when the excitation was changed from 448 to 454 and then to 456 nm, the emission maximum of the cation displayed shifts from 471 to 475 and 476.5 nm, respectively. This dependence of the emission spectra on the excitation wavelength is characteristic of the so-called red edge effect and implies that the solvent shell around the cation has reduced mobility for the reorientation of their dipoles around the excited-state fluorophore, resulting in a monotonic relaxation process.[54]

Time-Resolved Fluorimetry. C* ⇆ N* ⇆ M* Kinetics Studied through Global Compartmental Analysis. We studied the time course of the three excited species involved in the proton-transfer processes in the pH range between 1.1 and 3.0, and the kinetics of these excited-state reactions, by using time-resolved fluorimetry and the global compartmental analysis approach. The complete decay surface, described in Materials and Methods, was initially analyzed in terms of decay times and associated preexponential factors, although the kinetics of the excited-state processes involving C, N, and M were resolved through the one-step global three-compartmental analysis.

As cited before, very high acid concentrations were necessary to detect cation steady-state fluorescence emission. Nevertheless, in the following study, we have only used OG488 solutions at pH values between 1.1 and 3.0. In this biased pH range the processes of interest are quite conspicuous, since the three species (C, N, and M) are present in the ground state according to our previous absorption data, whereas only steady-state fluorescence emissions from N and M species are detected. At higher acid concentrations, additional effects, related to changes in media viscosity, ionic strength and water activity, are observed, and will be discussed later.

Individual and Global Analyses. Fluorescence decay traces, at every emission wavelength, pH and time scale, were individually fitted in terms of decay times and preexponential factors, and then, decay traces from solutions at the same pH were globally analyzed. In the usual global analysis approach, decay times were linked parameters over all the decay traces, while preexponentials were locally adjustable parameters.

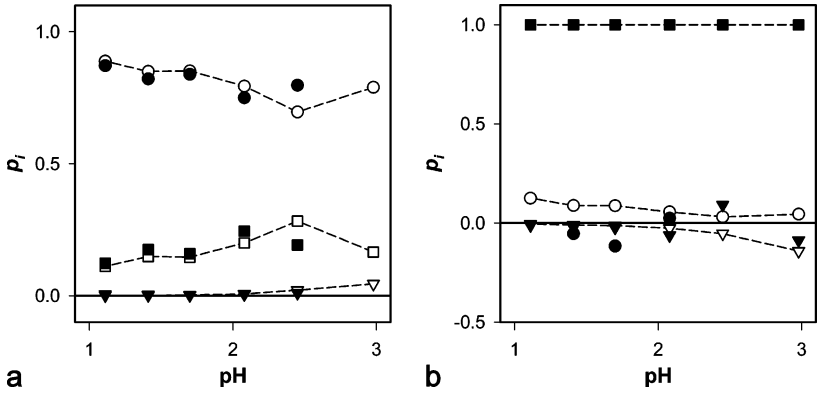

Figure 4. Preexponential factors associated with the longest (■), intermediate (▼), and shortest decay times (●), recovered from global analyses of decay traces, at the emission wavelengths 470 (a) and 580 nm (b), from OG488 in aqueous solution at pH values between 1.1 and 3.0. Also shown are the preexponential factors (-□-, -▽-, and -○- associated with the longest, intermediate, and shortest decay times respectively) calculated by means of the general equations (see Supporting Information), using the recovered values of $\tilde{\mathbf{b}}$, $\tilde{\mathbf{c}}$, and k_{ij} from the GCA. Note that in part a the factors are normalized according to $\sum p_i = 1$, whereas part b shows the ratios of each preexponential divided by the factor associated with the longest decay time, due to the presence of negative preexponential factors.

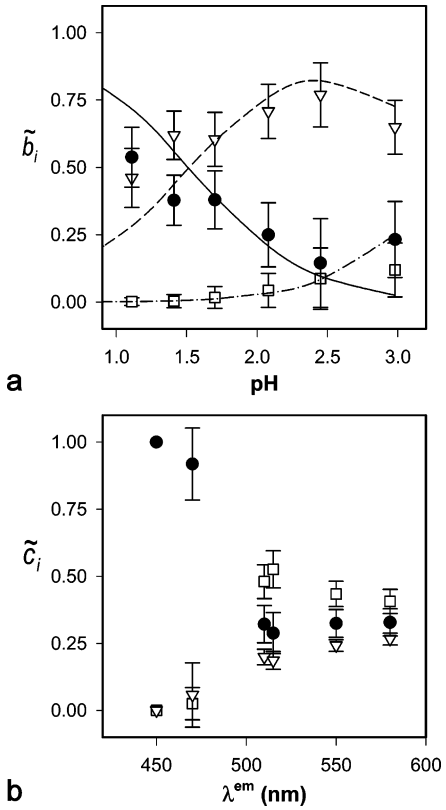

Figure 5. Excitation (a) and emission parameters (b) of the monoanion (□), neutral (▽), and cation (●), recovered by GCA of the fluorescence decay surface of OG488 aqueous solutions at pH values between 1.1 and 3.0. Lines in Figure 5a represent the $\tilde{b}_i$ values calculated using the general equations (see Supporting Information) and the ground-state results from our previous paper.

Individual analyses of traces acquired at the emission wavelengths of 450 and 470 nm provided good fits with biexponential functions, showing a short decay time (between 6 and 12 ps) and a longer one around 3.17 ns. The magnitude of the short decay time indicates the presence of a very fast process, which we assign to the deprotonation of OG488 cation. Since these wavelengths correspond to cation emission, the preexponential values associated with both decay times were positive. The magnitude of the short decay time is in the limit of resolution of our time-resolved fluorescence instrument. Nevertheless, the deconvolution method provided consistent results, showing negligible dependence with the initial guesses of the parameters, and an associated error of about 20% in the recovery of the shortest decay time.

At emission wavelengths of 510, 515, 550, and 580 nm (mainly N and M emissions), the individual analyses of decay traces also provided good double-exponential fits, but the two decay times were both in the nanosecond time range. The largest, around 3.17 ns, is common to those recovered at the emission wavelengths of 450 or 470 nm, and almost pH independent. On the contrary, the short decay time, which increases from 0.29 to 2.58 ns with increasing pH, is much longer than the 6−12 ps decay time recovered at 450−470 nm. This decay time showed a decreasing negative preexponential factor with increasing pH, whereas the preexponential associated with the largest decay time was always positive. The presence of the rise-time at these emission wavelengths indicates that the emitting species is/are formed in the excited-state process.

In general, three-exponential decay laws were the best models to fit globally the experimental decay traces from solutions at the same pH. The decay times from the global analyses vs pH are represented in Figure 3 as symbols. Figure 4a shows the normalized associated preexponential factors vs pH at $\lambda^{em} =$ 470 nm (filled symbols). At this wavelength the preexponential values associated with the intermediate decay time are close to zero, which explains the acceptable double-exponential fits from individual analysis. Figure 4b shows the associated preexponential factors vs pH at the emission wavelength of 580 nm (filled symbols). It can be seen that the factor associated with the shortest decay time was poorly recovered, showing no trend when represented vs pH and randomly varying between negative and positive values.

Global analysis is more powerful than individual analysis as it permits analysis of a fluorescence decay surface recorded at different wavelengths, taking advantage of the relationship between different decay traces over the complete decay surface. Nevertheless, in the application to the OG488 system, global analysis introduces fluorescence decay times that are poorly recovered at the emission wavelengths in which individual analyses were well fitted by biexponential functions. When these decay times are long enough, as is the case of the intermediate decay time, the associated preexponentials result in a monotonic near to zero value, for instance at $\lambda^{em} \leq 470$ nm. On the contrary, if the decay times are short, a small error in these poorly recovered decay times originates a considerable deviation of the associated preexponential values. These features give rise

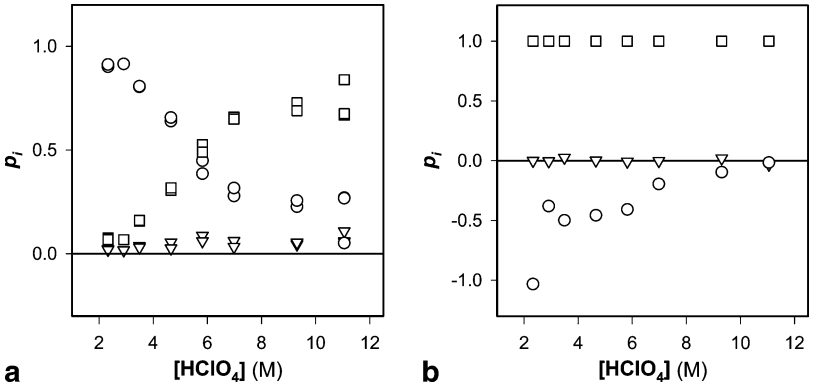

Figure 6. Preexponential factors associated with the longest (□), intermediate (▽), and shortest decay times (○) from global analyses, as a function of the perchloric acid concentration, at the emission wavelengths of 450 (a) and 550 nm (b). The factors at 450 nm are normalized according to $\sum p_i = 1$, whereas those from decays at 550 nm are the ratios of each preexponential divided by the factor associated with the longer decay time, due to the presence of negative preexponential factors.

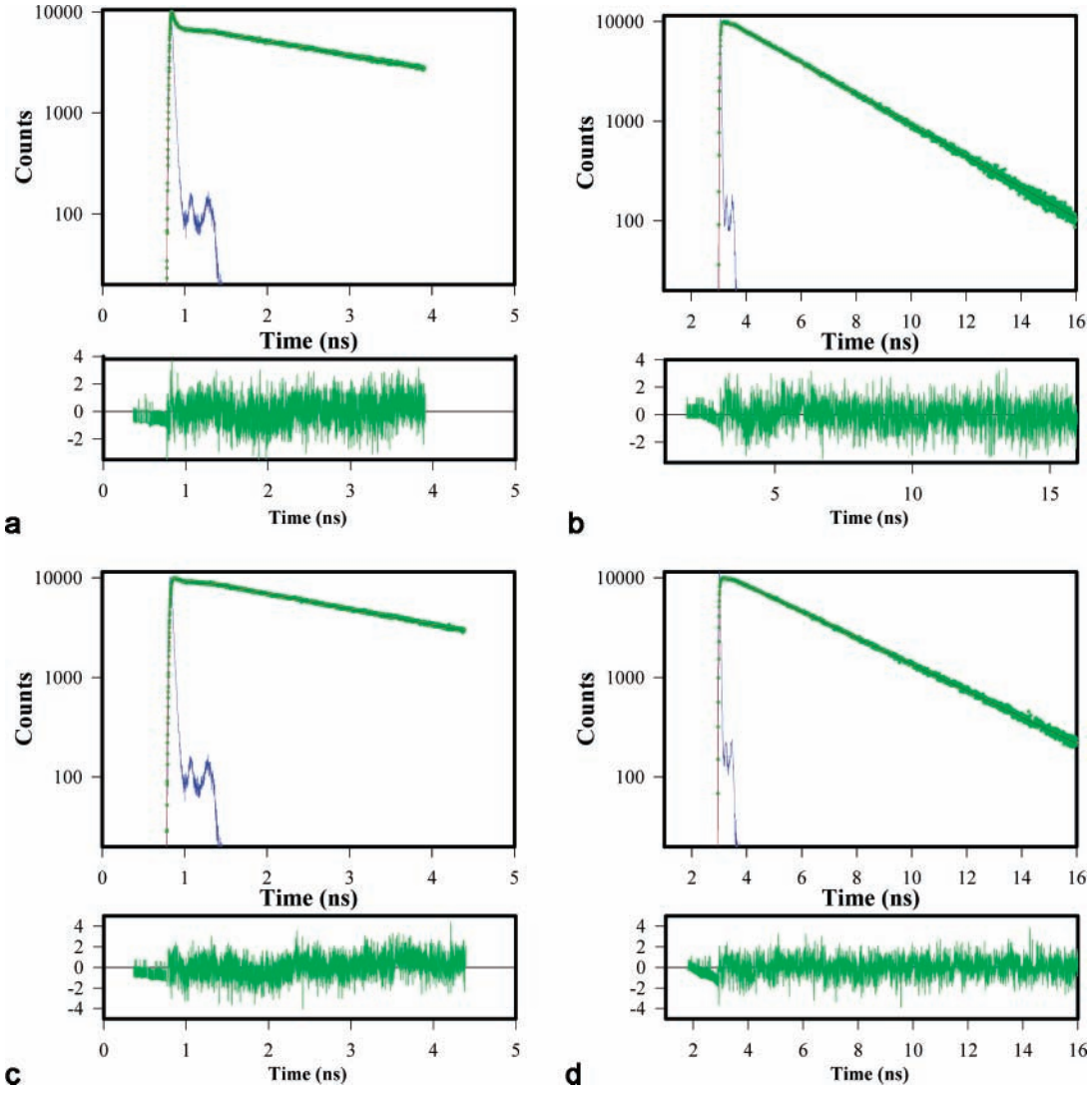

Figure 7. Fluorescence decay traces (green) of OG488 aqueous solutions ($\lambda^{ex} = 420$ nm) at (a) [HClO$_4$] = 2.3 M, $\lambda^{em} = 470$ nm, and 1.22 ps/channel, $\chi^2 = 1.062$; (b) [HClO$_4$] = 5.8 M, $\lambda^{em} = 550$ nm, and 5.94 ps/channel, $\chi^2 = 1.108$; (c) [HClO$_4$] = 5.8 M, $\lambda^{em} = 450$ nm, and 1.22 ps/channel, $\chi^2 = 1.148$; and (d) [HClO$_4$] = 11.1 M, $\lambda^{em} = 510$ nm, and 5.94 ps/channel, $\chi^2 = 1.014$. The instrument response function (blue line) and the triexponential fitting (red line) are also shown. The plots underneath show the weighted residuals from the fits.

to the random distribution observed for the recovered preexponentials associated with the shortest decay times at $\lambda^{em} \geq 510$ nm.

At pH values between 0.3 and 1.1, the intermediate decay time decreases with the increase in acid concentration, until it reaches values of the same order as the shortest decay time. At these acid concentrations, the best decay law to globally fit the decay traces was thus a biexponential function, whereas the individual analyses of traces at $\lambda^{em} \geq 510$ nm were monoexponentials. The preexponential factor associated with the shortest

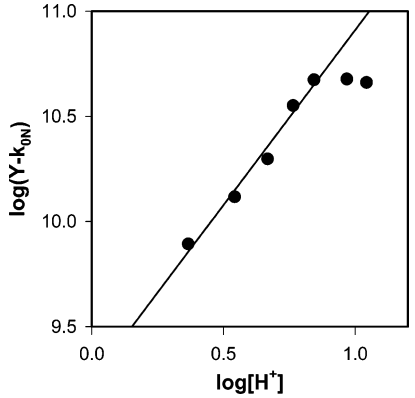

Figure 8. Plot of $\log(Y - k_{0N})$ vs $\log[H^+]$. The linear regression includes only the values up to the saturation.

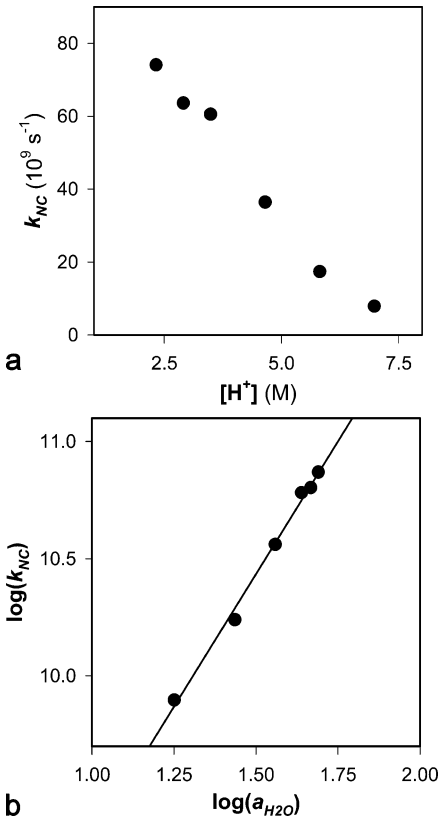

Figure 9. (a) Estimated k_{NC} values at different perchloric acid concentrations. (b) Logarithmical plot of the k_{NC} values of Figure 9a vs water activity (in the molar scale) as a representation of the free amount of water acting as proton acceptor.

decay time is thus recovered with very low reliability and accuracy.

Global Compartmental Analysis. The absorption, steady-state, and time-resolved fluorescence results provided above suggest the presence of a coupled kinetic system consisting of three ground- and excited-state species. Therefore, we propose Scheme 2 showing the ground-state equilibria and excited-state reactions taking place. Because of the high complexity of the system, at pH values in which the reprotonation reactions are not negligible, we used GCA to solve the excited-state kinetics. The GCA approach has shown several advantages in this sort of systems.[8]

The fitting process assumes the recovery of seven rate constants, depicted in Scheme 2, the normalized excitation parameters of M and N ($\tilde{b}_M$(pH) and $\tilde{b}_N$(pH)) at each $[H^+]$, and

SCHEME 1. Acid−Base Ground-State Equilibria, Equilibrium Constants (pK_i), and Prototropic Species of OG488 in Aqueous Solution

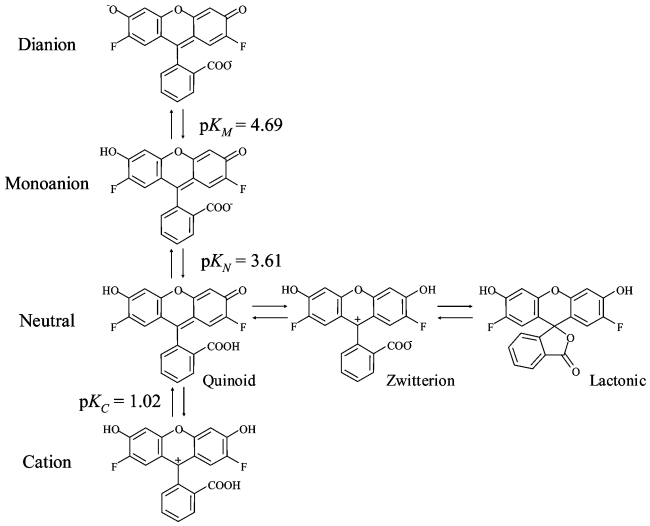

SCHEME 2. Kinetic Model of the Two Consecutive Excited-state Proton Transfer Reactions between Monoanion (M), Neutral (N), and Cation (C) of OG488 in Aqueous Solution

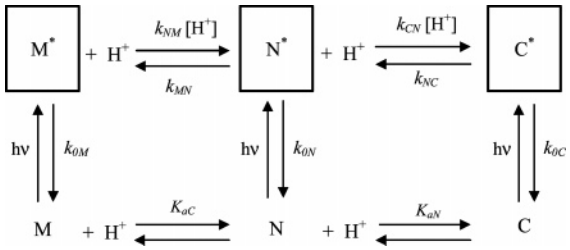

the normalized emission parameters of M and N ($\tilde{c}_M(\lambda^{em})$ and $\tilde{c}_N(\lambda^{em})$) at each emission wavelength. The theory and details of the GCA fitting process are provided as Supporting Information.

In the GCA, the availability of a priori information provides certainty of recovering unique values for adjustable parameters and is a tool for verifying the coherence of results from global compartmental analysis. In our study, we have the following information at our disposal: (1) according to steady-state spectra, neutral and monoanionic species do not emit at 450 nm ($\tilde{c}_M$ (450 nm) = $\tilde{c}_N$(450 nm) = 0), and emission at 470 nm is very slight; (2) the excitation parameters can be calculated according to previous absorption data and ground-state results, giving the possibility of comparing recovered $\tilde{b}_i$ values with those calculated; (3) excitation of OG488 monoanion at the $[H^+]$ used is almost zero in most of the decays; (4) we reported elsewhere[4] a value for k_{0M} of $(2.94 \pm 0.01) \times 10^8$ s^{-1}; (5) the presence of OG488 dianion can be completely ignored, since at the pH values used in this work it does not exist in the ground-state and its formation from M is not favorable in the absence of a suitable proton acceptor/donor, such as acetate buffer.[4]

The recovered rate constants, species lifetimes, and calculated pK_a^* are shown in Table 1. Using these rate constant values, we calculated the decay times according to the general equations of the compartmental model (see *Supporting Information*). Figure 3 shows the excellent agreement between calculated decay times (lines), and the decay times recovered from global analyses (symbols). Finally, Figure 5 shows the recovered excitation ($\tilde{b}_i$) and emission ($\tilde{c}_i$) parameters. As can be seen in

TABLE 1: Recovered Rate Constant Values from Global Three-Compartmental Analysis of the Fluorescence Decay Surface of OG488 Aqueous Solutions at pH between 1.1 and 3.0

k_{0M} (s^{-1})	$(3.07 \pm 0.04) \times 10^8$	$\tau_M = 1/k_{0M} = 3.26 \pm 0.04$ ns
k_{0N} (s^{-1})	$(3.14 \pm 0.03) \times 10^8$	$\tau_N = 1/k_{0N} = 3.18 \pm 0.03$ ns
k_{0C} (s^{-1})	$(4.5 \pm 0.8) \times 10^8$	$\tau_C = 1/k_{0C} = 2.2 \pm 0.4$ ns
k_{MN} (s^{-1})	$(3.9 \pm 0.1) \times 10^7$	$pK_N^* = 3.14 \pm 0.05$[b]
k_{NM} ($M^{-1}\ s^{-1}$)	$(5.4 \pm 0.6) \times 10^{10}$	
k_{NC} (s^{-1})	$(1.04 \pm 0.04) \times 10^{11}$	$pK_C^* = -1.79 \pm 0.08$[c]
k_{CN} ($M^{-1}\ s^{-1}$)[a]	$(1.7 \pm 0.1) \times 10^9$	

[a] Recovered by linear fitting of the individual k_{CN}' (see Supporting Information for details). [b] Calculated using $K_N^* = k_{MN}/k_{NM}$. [c] Calculated using $K_C^* = k_{NC}/k_{CN}$.

this figure, the agreement between recovered $\tilde{b}_i$ values (symbols), and those predicted by our previous absorption data, shown as lines, is also very good. Nevertheless, the cation $\tilde{c}_C$ values seem to be overestimated with respect to the neutral $\tilde{c}_N$ values at $\lambda^{em} \geq 510$ nm, since, from Figure 2, it can be observed that N has higher emission efficiency than C, in the wavelength range between 510 and 580 nm. By using the recovered values of k_{ij}, $\tilde{b}_i$, and $\tilde{c}_i$, the preexponential factors were calculated and are shown as blank symbols in Figure 4. Figure 4a shows a good agreement between the values recovered in global analyses and the calculated values. On the contrary, a worse coincidence was found for preexponential factors at $\lambda^{em} \geq 510$ nm. The calculated values for the preexponential associated with the shortest decay time were always positive. This is unexpected since the shortest decay time mainly reflects the fastest process, i.e., the deprotonation of the cation to neutral, and from Figure 2 the C emission at 580 nm is smaller than the N emission, the preexponential values associated with the shortest decay times should be thus negative. The overestimation of the 580 nm $\tilde{c}_C$ values recovered from GCA explains the positive value of this preexponential factor. Simulations of the preexponential factors using different values of the $\tilde{c}_i$ parameters, including the condition $\tilde{c}_C/\tilde{c}_N$ ratio < 1, confirmed a negative preexponential associated with the shortest decay time, as it would be foreseen by observation of the steady-state fluorescence spectra. The inaccuracy of the analysis method for recovering the cation associated $\tilde{c}_i$ parameters at $\lambda^{em} \geq 510$ nm arises from the fact that at $\lambda^{em} \geq 510$ nm the individual analyses of decay traces did not show the shortest decay time. Nevertheless, the shortest decay times were more accurately recovered from decay traces at $\lambda^{em} \leq 470$ nm, and the recovery of the relevant kinetic constants has not been affected by the inaccuracy of the spectral emission parameters.

Time-Resolved Fluorescence Measurements of OG488 in Very Acidic Media. As mentioned above, the steady-state emission of the cationic form is only detected at acid concentrations above 2.3 M. A complete fluorescence decay surface of OG488 aqueous solutions at this $[H^+]$ range (between 2.3 and 11.1 M) was collected. The decay traces were analyzed using the global analysis approach of decays at the same acid concentration. Three-exponential decay laws were the best functions to fit the decay traces at emission wavelengths 450 and 470 nm, whereas traces at 510, 550, and 580 nm were mainly mono- or biexponentials. The global analyses provided three decay times, two of them between 8 and 165 ps and a longer one around 3 ns. The recovered decay times in the global analyses are shown in Figure 3, and the preexponential factors at the emission wavelengths of 450 and 550 nm are shown in Figure 6. At 450 and 470 nm, the shortest decay time showed large amplitude, which decreases with increasing acid concentration. On the other hand, the longest decay time showed increasing associated amplitude with increasing acid concentration. The intermediate decay time always showed a very low poorly resolved associated preexponential. From the decay traces at $\lambda^{em} \geq 510$ nm, the longest decay time was recovered with a positive well-defined preexponential factor, whereas the shortest decay time generally showed a negative preexponential factor. The preexponential factors associated with the intermediate decay time were scarcely recovered and showed dependency on the initial guess. Figure 7 shows some experimental decay traces, the convoluted global fitted function, the weighted residuals, and the instrument profile.

The three-exponential decay laws in this $[H^+]$ range and the unusual trends of the decay times make the proposed model for the C* ⇆ N* ⇆ M* reactions insufficient. These extremely acidic media show some special characteristics that hinder the study of the excited-state processes. At such a high acid concentration some other effects could alter the excited-state behavior of the OG488 species. These will be considered in the Discussion.

We have also carried out some measurements of fluorescence emission decay traces of OG488 in 9.4 M perchloric acid solution, as a function of the temperature. Temperature does not appreciably alter the fluorescence emission rate. However other processes such as quenching, viscosity of the solution, or nonradiative deactivation paths are considerably affected by temperature variations. We recorded the decay traces using the nanosecond instrument described in the Materials and Methods section and under the experimental conditions described there. Since the time resolution of the instrument is not high enough, only the largest decay time was recovered when fitting the traces. The decay traces thus follow monoexponential decay laws (showing χ^2 values below 1.098) since the shorter decay time(s) are completely embedded within the excitation source profile channels. A slight decrease in the recovered decay time was obtained when temperature was increased. The decay time was 3.19 ± 0.02 ns at 278 K, and progressively diminished giving decay times of 3.15 ± 0.02 ns at 293 K and 3.04 ± 0.02 at 318 K. We remark once again that these decay traces are not actually monoexponential functions and the largest decay time, recovered here, shows a main contribution of the cation deactivation rate.

Discussion

The absorption spectra of OG488 solutions at pH values below 3 have been well predicted by our previous results regarding ground-state pK_a and ϵ_i. Nevertheless, some special features have been described at very high acid concentrations. A blue shift of the cation absorption spectra with increasing perchloric acid concentration has been found. This shift is continuous with changing acidity, showing no isosbestic point. A similar blue shift of the absorption spectra in extreme acidic media was previously described for fluorescein, the stem probe of OG488, and 2′,7′-dichlorofluorescein, a fluorescein derivative with chlorine substituents similar to OG488.[3] In OG488, we found that the absorption maximum shifts 7.5 nm, from 437.5 to 430 nm at $[HClO_4] = 11.1$ M. Leonhardt et al.[3] found a 5 nm blue-shift of the fluorescein absorption maximum in perchloric acid (from 436 nm at 0.50 M to 431 nm at 7.40 M), a shift of 3 nm in sulfuric acid ($\lambda^{max} = 433$ nm at 10 M), but no shift in nitric acid (absorption maximum remains invariable at 436 nm at $[HNO_3] = 7$ M). Similar results were found for 2′,7′-dichlorofluorescein, whose absorption maximum shifts 7 nm in perchloric acid (from 448 nm at 0.50 M to 441 nm at 11.70 M), and 4 nm in sulfuric acid 10 M ($\lambda^{max} = 444$ nm).[3] The blue shift of the absorption spectra in extreme acidic media

has also been described by other authors in fluorescein[19] and uranine (fluorescein salt).[18] These authors proposed the existence of dicationic forms (in which the oxygen bridge of the xanthene moiety would be protonated) at very high sulfuric acid concentration. The dicationic forms would cause the blue shift in the absorption spectra and show a different emission band centered at 495 nm, at 18 M H_2SO_4. Although in OG488 we found a blue shift in the absorption spectra, we have not found evidence for a dicationic species existing in solution, since only the emission band with maximum at 471 nm has been observed. As OG488 is a stronger acid than fluorescein, due to fluorine substituents, the possible dication would be much more hindered. The observation of a red shift of 5.5 nm in the wavelength of the maximum fluorescence emission, when the fluorophore is excited at wavelengths toward the red edge of the absorption band, implies that dipolar relaxation time for the solvent shell around fluorophore is comparable to its fluorescence lifetime. Therefore, this red edge effect also implies slow rates of solvent relaxation at the highest acid concentrations in which hydration of the protons hinders the free reorientational motion of the solvent dipoles around the excited-state fluorophore. Hence, we are inclined to think in polarizability effects that affect to the solvent relaxation. A similar bathochromic shift with decreasing acid concentration was found for the cation of 6-hydroxyquinoline,[22,55] another cationic strong photoacid. Bardez et al. also suggested environmental effects as the cause of the spectral shift.[22] Medium effects on the absorption or emission spectra (shifts, alteration of fluorescence efficiency, etc.) are a frequent problem in absorption and fluorescence measurements of dyes in varying high concentration acid or electrolyte solutions.[26,54,56] The spectral shifts have been frequently correlated with the solvent properties, such as polarity, solvation ability, acidity or basicity, and so forth. For instance, a strong photoacid such as HPTS was found to be a good polarity probe for concentrated sulfuric acid solutions.[57]

With reference to the excited-state kinetics studied in the present work, the system of consecutive ESPT reactions of OG488 cation, neutral, and monoanion in the pH range 1.1−3.0 has been one of the most complex solved to date to the best of our knowledge. Only a few excited-state reactions involving more than two excited species have been solved,[13−17] and a few tricompartmental systems have been successfully analyzed,[11,12] but the system solved here is even more complex, due to the wide spectral overlap and the high acidity of one of the species. In addition, the usefulness of the global compartmental analysis for unravelling complex kinetics has also been shown in this work.

The extremely strong photoacid behavior of C has been demonstrated by means of both steady-state and time-resolved fluorescence emission measurements. A deprotonation rate constant of $(1.04 \pm 0.04) \times 10^{11}$ s^{-1} was recovered. This is one of the highest values obtained for the deprotonation to water of a photoacid to date. A deprotonation rate of the same order of magnitude, $(1.4 \pm 0.3) \times 10^{11}$ s^{-1}, was recovered for the cation 7-hydroxy-4-methylflavylium,[58] another cationic photoacid. When the recovered value is compared to the value obtained by Shah and Pant for deprotonation of fluorescein cation (3.5×10^{10} s^{-1}),[19] the enhanced acidity of OG488 due to fluorine substitution is again displayed. It is instructive to compare the dissociation rates with other cationic photoacids, since these are known to behave thermodynamically quite differently with respect to neutral photoacids.[20] Another point of interest regarding the excited-state reactions of *C* is the relatively low value of the reprotonation rate constant ($k_{CN} = (1.7 \pm 0.1) \times 10^9$ M^{-1} s^{-1}). This value is lower than typical values for diffusion-controlled reactions in water.[25] This low value indicates a hindered reprotonation reaction of the neutral form, and will be discussed later on. Low reprotonation rates, even the absolute absence of reprotonation reaction, are common in strong and cationic photoacids.[22] The recovered kinetic constant values provide an apparent excited state $pK_a^* = -1.79$, perhaps too low to solely observe the cation emission at $[HClO_4] \approx 10$ M. However, this pK_a^* is an apparent value, and the activity coefficients at the high acid concentrations are very far from 1.

The other consecutive excited-state reaction N* ⇆ M* showed a pK_a^* of 3.14 ± 0.05 (calculated by $K_a = k_{MN}/k_{NM}$). This value is significantly higher than the value recovered by means of steady-state fluorescence measurements from our previous paper (2.67).[4] The value of 2.67 was obtained as the best estimation fitting globally I_F vs pH curves, and it should be considered as an apparent pK_a^*. Because of the spectral coincidence between emission of N and M, one should be very cautious with the interpretation of this pK_a^* value. On the other hand, the value provided in this work, 3.14, has been obtained from kinetics measurements and estimations of the kinetic rate constants, and is thus more reliable. The pK_a^* value is, in both cases, lower than the ground-state pK_a (3.61),[4] thus meaning that the neutral species becomes slightly more acidic upon excitation. The deprotonation rate constant value ($(3.9 \pm 0.1) \times 10^7$ s^{-1}) does not entail a great contribution to the deactivation processes, but the reprotonation reaction ($k_{NM} = (5.4 \pm 0.6) \times 10^{10}$ M^{-1} s^{-1}), which showed a typical diffusion-control value,[25] mainly controls the excited-state process between both species in this pH range. It is also interesting that the N and M forms showed a very similar deactivation rate. This results in the longer decay time being essentially invariable in this pH range, and suggests the same chromophoric group for the two species. The similarity of the N and M emission spectral parameters recovered also supports this idea. This would thus mean that the neutral exists in the quinoid form.

Deprotonation of N* to M*, occurring in the carboxylic acid group, is in apparent contradiction with the known fact that aromatic carboxylic acids are weaker acids in the excited state. Normally, the decrease in acidity follows the increase in negative charge of the hydroxyl oxygen of the carboxyl group resulting from electronic excitation (more precisely, the "ionic O−H bond strength" $z_O z_H / r_{O-H}$).[59] In the case of OG488, however, the benzoic moiety is not "excited" (at 420 nm) due to the near perpendicularity of benzyl and xanthene moieties. From AM1 calculations the S_1 state of N actually is a locally excited (LE) state of the xanthene ring, and, as a result, the benzoic moiety only suffers from through-bond and/or through-space inductive effects upon excitation of the xanthene. Interestingly, these effects cause a slight *decrease* of the ionic bond strength of the hydroxyl oxygen of the carboxyl group, thus predicting an *increase* in the carboxylic group acidity upon excitation. Thought the calculations also predict a moderate increase in acidity of the xanthene hydroxyl group, the experimental observation is that deprotonation of the second hydroxyl group only occurs at higher pH values and in the presence of a suitable proton acceptor, such as acetic acid.[4] It seems that the neutral zwitterionic form disappears in the excited-state, as it was also described in fluorescein.[10,18,19] The absence of the zwitterionic form in the excited-state is expected due to its minimal contribution in the ground state. Moreover, the deprotonation of C is likely to occur through the hydroxyl group in the xanthene moiety (which is excited in the visible

range). The ejection of the proton of the hydroxyl group generates a charge separation within the xanthylium ring, which is rapidly compensated by a rapid electronic redistribution. The positive pole in the moiety facilitates the charge transfer leading to the quinoid neutral form. This process resembles the charge transfer after deprotonation of hydroxyquinolinium cations,[22,60] and is responsible for the low value of the reprotonation rate constant as a result of the neutral quinoid form stabilization. In hydroxyquinoline cations, the consecutive electron transfer after deprotonation, found to be faster than 450 fs,[60] causes the absence of back-reaction and an irreversible deprotonation.[22] In contrast, the deprotonation of C to form the zwitterion is very unlikely, since it would imply either the deprotonation of the carboxylic acid linked to the unconjugated ring, excited by UV light but not in the visible range, or a double proton transfer, one intermolecular resulting in the quinoid form, followed by another intramolecular proton-transfer resulting in the zwitterion. Finally, we found a good agreement between the recovered lifetime for M in the present work ($1/k_{0M} = 3.26 \pm 0.04$ ns) and our previous reported value (3.40 ns).[4]

It is worth noting that the GCA approach uses time-invariant rate constants, leading to exponential kinetics for the reactions. This is known to be an approximation in diffusion-influenced reactions. The reactions studied in the present work show one of the reactants (H^+) in great excess (pseudo-unimolecular regime), and they are subject to the Smoluchowski equation.[33,34] This theory predicts nonexponential decays for this type of reaction, even when diffusion does not show a striking significance. The expected decays are markedly nonexponential at the beginning, because of the time dependence of the rate constants, which decrease from their initial intrinsic value up to a steady-state. Then, after a quasi-exponential phase, the decay traces ought to follow an asymptotic power law ($t^{-3/2}$) due to the reversible dissociation of the geminate pair. Nevertheless, in the decay traces from solutions at pH values between 1.1 and 3.0 recorded in our instrument, the exponential approach lead to excellent results. We did not detect the asymptotic behavior at long times, as well as the shortest decay time described very well the initial times of the decay traces. The shortest decay time was in the resolution limit of the instrument, so this might be the cause of the loss of the nonexponential behavior. A further discussion on the decay traces at higher acid concentration and the diffusion influenced kinetics is issued in the following section.

Considerations on the Kinetics of the Excited-State Processes in Concentrated Acid Media. The excited-state kinetics of the ESPT reactions C* ⇆ N* ⇆ M* have been well described and suitably solved in the previous section, in a pH range between 1.1 and 3.0, by means of a global three-compartmental analysis of the fluorescence decay surface. Nevertheless, other interesting processes seem to take place at the $[H^+]$ range between 2.3 and 11.1 M. In this part of the work, we will consider some well-known effects on the excited-state processes which occur in these high acidity media and correlate these effects with the time-resolved fluorescence emissive behavior of the OG488.

When perchloric acid concentration is around 0.1 M decay traces were well globally fitted by triexponential functions, the amplitude related to intermediate decay time was very short and tended to zero when the acid concentration increased. Next, decay traces become fittable with biexponential functions, since the two shorter decay times converge. When perchloric acid concentration was increased in the 2.3 to 11.1 M range, biexponential decay laws were no longer adequate and the decay traces could only be well fitted with triexponential functions again, with the appearance of an unexpected intermediate lifetime of around 100 ps matching the tail region of the instrumental response of our picosecond device. Moreover, in these triexponential functions, the largest decay time showed an unusual tendency to diminish and then to increase, while the shortest also had an unusual tendency to increase slightly. Multiexponential (four-exponential) fittings also gave good results, and a new decay time of similar magnitude to the intermediate one was recovered, without alteration of either the shortest or the longest decay time values. The inadequacy of biexponential fits is a frequent event in decays involving ultrafast deprotonations, which may result in nonexponential decay traces, possibly confused with multiexponential decay laws. As mentioned previously, diffusion-influenced reactions may show transient effects, resulting from time-dependent rate constants, following the Debye−Smoluchowski theory. The decay of the photoacid is expected to follow very well the convolution kinetics approach[45] at low and intermediate times, and change to a power law asymptotically. This behavior has been observed in some photoacids in acidic aqueous solutions.[43,44] Solntsev et al. suggested a deconvolution/smoothing procedure through a four-exponential fitting so they could test the validity of the convolution kinetics approach and the asymptotic $t^{-3/2}$ decays of 2-naphthol-6,8-disulfonate in acidic media.[44] The treatment of our decay traces in very acidic media in terms similar to those used by Solntsev et al. did not show a power-law decay at long times. The decays followed, nevertheless, a purely exponential decay law until the noise became higher than the signal. Moreover, an asymptotic power law $t^{-1/2}$ for the associated base has been described.[61] Unlike these results, our decay traces for the acid (450 nm) and the base form (550 and 580 nm) showed exponential behavior and the same long decay time for both species, thus confirming the validity in this time range of the coupled differential equations leading to the exponential approximation. We fitted our decay traces of solutions at very high $[H^+]$ using tri- and tetraexponential decay laws, and we could assume the shortest and intermediate decay times are influenced by transient effects, resulting in the fluorescence signal changing from an initial exponential decay to a long-time power law. Unfortunately, our picosecond device is not able to accurately resolve the possible nonexponential distribution observed around 100 ps, since the instrumental response profile showed secondary peaks in a crucial time region (see decay traces in Figure 7). Furthermore, the impossibility of acquiring decay traces in the geminate recombination limit (neutral pH), due to the presence of other more basic species, does not allow us to apply the Debye−Smoluchowski or convolution kinetics approaches.

In the case of higher acid concentrations, the global compartmental analysis software has not been useful enough since the variability of rate constants is not included in the available (up to date) compartmental models. Likewise, the classic procedures of recovering the rate constant values have not provided a solution due to the special characteristics of the complete fluorescence decay surface recorded (three-exponential global fittings, poor resolution recovery of preexponential factors, unusual tendencies in the decay times, etc.). At high acid concentrations some other additional issues arise, causing variations in the rate constants with acid concentration and making the kinetic model insufficient to explain all the features of the fluorescence decay traces. In the following discussion, these variations are quantified and correlated with physical

effects, giving an overview of the processes taking place during the lifetime of the excited-species.

Since the protonation of M is very favorable at these high proton concentrations our first step was to restrict the excited-state kinetic model to a two-state excited-state reaction. This is presumably correct, taking into account the relatively low value of the deprotonation of neutral species ($k_{MN} = 3.9 \times 10^7$ s^{-1}), and the higher value of the protonation of M ($k_{NM} = 5.4 \times 10^{10}$ M^{-1} s^{-1}), which implies that only 1% of the excited C will form M. The system is thus reduced to the coexistence of N and C species. This also agrees with our experimental results which show a very low preexponential associated with the intermediate decay time at these high proton concentrations.

In a first step, we have applied a kinetic approach by which the time evolution of the neutral emission, $I_N(t)$, is given by[62]

$$I_N(t) = k_{NC}[I_C(t) \otimes e^{-\gamma t}] \quad (1)$$

where the symbol $\otimes$ represents convolution, $I_C(t)$ is the emission of C, and $Y = (k_{0N} + k_{CN} \times [H^+])$. This approach is usable assuming that *C* is the only excited species and there is no spectral overlap at the emission wavelengths of the acid and the base. The former is fulfilled according to the ground-state equilibria, but the latter is not, at 550 and 580 nm. Nevertheless, the cation contribution to emission at these wavelengths is almost negligible. The procedure evaluates the N* loss processes ($k_{0N} + k_{CN} \times [H^+]$) by the deconvolution of the decay of N (at 550 and 580 nm) from the decay of C (at 450 nm). This kind of analysis should provide single-exponential fits, with a decay time equal to $\tau_Y = Y^{-1}$. This type of convolution kinetics is strongly recommended when transient effects, FRET, quenching, etc. are present.[62] It has been successfully applied to the study of such a strong photoacid as 7-hydroxy-4-methylflavylium cation,[58] when other classical methods of analysis failed. According to the convolution kinetics, the plot of the $1/\tau_Y$ vs $[H^+]$ should be linear, when simple two-state excited-state kinetics apply. In contrast, our results showed a clear nonlinearity, with a saturation maximum value at acid concentrations above 7.0 M. These features clearly indicate that the rate constants are $[H^+]$-dependent. The plot of $\log(Y - k_{0N})$ vs $\log[H^+]$ showed a good linearity up to the saturation value (Figure 8). The intercept of the linear regression of the corresponding points ($r^2 = 0.98$) provided a value for k_{CN} of $(1.7 \pm 0.4) \times 10^9$ M^{-1} s^{-1}, which is in good agreement with the value obtained in the previous section by means of GCA (Table 1). However, the slope of the linear regression was 1.7 ± 0.1, which indicates a enhanced reprotonation of the neutral at these high $[H^+]$.

We have also studied the possible variations in the deprotonation rate of C. In our GCA approach, we considered k_{NC} as a pseudo-first-order deprotonation rate constant, but this could not be a correct assumption at the high $[H^+]$ range. The necessary formation of water clusters acting as acceptors of the proton produced by deprotonation of photoacids in the excited state has been well established,[27−32,63−65] and at very high acid concentrations, the majority of the water molecules have been commonly thought to be within the hydration cages around ions, resulting in a loss of the effective proton acceptors available for deprotonation of the photoacid. Hence, the rate of the deprotonation-to-solvent of the photoacid depends on the concentration of free water clusters,[63] resulting in the deprotonation rate not actually being a pseudo-first order reaction. This effect has also similarly been found and described in water: organic solvents mixtures.[29,41] Solntsev et al. in their procedure for deconvolution/smoothing of the decay traces[44] assigned the shortest decay time to the deprotonation rate of 2-naphthol-6,8-disulfonate, noting that this decay time was basically independent of the acid concentration. In our case, the shortest decay time showed a marked increase with increasing acid concentration (varying from 8 ps at $[H^+] = 2.3$ M to 73 ps at $[H^+] = 11.1$ M), which means a decrease in k_{NC} with $[H^+]$ (shown in Figure 9a). This decrease can be explained on the basis of the reduction in the number of proton acceptors (water clusters) with increasing $[HClO_4]$. The loss of free water effect in the deprotonation rate could be roughly represented by the empirical expression[63] $k_{NC} = k'_{NC}\,(a_{H_2O})^n$, where k'_{NC} is the dissociation rate constant at infinite dilution, a_{H_2O} the water activity, and n is an empirical parameter which may be related to the size of the water clusters accepting the protons. We used the experimental activity values for $HClO_4$ concentrated solutions[66] in the logarithmical plot of k_{NC} vs $\log(a_{H_2O})$ (Figure 9b). A good linearity ($r^2 = 0.99$) can be seen, with a slope $n = 2.3 \pm 0.1$, which represents the number of water molecules in the proton-accepting water cluster. This number is similar to values found for other strong photoacids, such as cyanonaphthols[28] or 4-hydroxy-1-naphthalenesulfonate,[29] and agrees well with the value found by Bardez et al. (2.75) for the cationic photoacid 6-hydroxyquinoline.[22] More importantly, this value is consistent with the idea of a water dimer as the most important solvation complex of the proton in concentrated acid solutions and with Pines and Fleming's assumption that the proton transfer to solvent on cationic photoacids is governed by proton solvation.[24] The intercept of the plot provided the limit value at high dilution for k_{NC} ($=k'_{NC}(a_{H_2O}^{\text{diluted}})^n$) of 1.0×10^{11} s^{-1}, a value very similar to that recovered by GCA (1.04×10^{11} s^{-1}). We note that the striking decrease in k_{NC} causes the unusual tendency of the shortest decay time to increase with increasing acid concentration.

Nevertheless, the correction described above is not enough to understand the unusual trend of the longest decay time (see Figure 3). The tendency of this decay time to rise at higher acid concentrations can only be explained by the following points: (1) the assumption of a new prototropic species with a shorter deactivation rate, as stated by Pant et al.,[18] or (2) by a decrease of the deactivation rate constant of the cation with increasing acid concentration. Here, we note that Pant et al.[18] observed a similar behavior of the longest decay time in fluorescein solutions at high H_2SO_4 concentration. This work was carried out by using a nanosecond flash lamp. They thus obtained well fitted monoexponential functions, as we did in the experiments at different temperatures using our nanosecond flash lamp. The authors proposed the existence of a dicationic species for explaining the absorption and fluorescence emission behavior. As previously mentioned, we did not find evidence for the presence of a dication of OG488 in aqueous solution either by means of absorption or steady-state fluorescence. Intuitively, we can assume that if the dication exists, it would be even more acidic in the excited state than the cation. Its formation would thus not be favorable. Consequently, we are inclined to consider variations in k_{0C}, due to medium effects, which are also reflected in the progressive blue shift in the absorption spectrum and by the red edge effect at the highest acid concentration.

We estimated k_{0C} at each $[H^+]$, taking into account the known values of the reprotonation rate constant (from Figure 8) and the deprotonation rate decreasing with water activity (Figure 9b). In this approach, we ignored the effects of the slow rates of solvent relaxation on the recovered decay times at different emission wavelengths, since the red edge effect was only observed at the highest perchloric concentration. The recovered

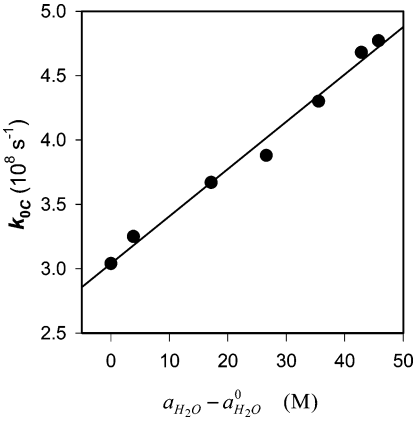

Figure 10. Modified Stern−Volmer plot of the recovered deactivation rate constants for the OG488 cation as a function of the water activity (representing the "free" water amount).

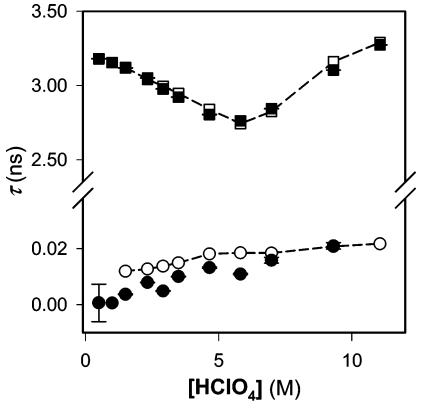

Figure 11. Comparison of the shortest and longest decay times recovered from global analyses (■ and ●) and the calculated decay times (-□- and -○-) assuming a simple two-state excited-state model and the approximations described in the text: $k_{0N} = 3.14 \times 10^8$ s^{-1}, $k_{0C} = [0.304 + 3.7 \times 10^{-3} (a_{H_2O} - a^0_{H_2O})] \times 10^9$ s^{-1}, $k_{NC} = 1.0 \times 10^7 (a_{H_2O})^{2.3}$ s^{-1}, and $k_{CN} \times [H^+]$, the values recovered as $Y - k_{0N}$ (see text for details).

k_{0C} values were continuously decreasing with the increase in acid concentration. This behavior resembles that of other xanthylium cations[49] (the same type of cation than fluorescein or OG488) and other dyes[47] which are known to be quenched by free water molecules. In this quenching, as the acidity of the solution increases, the amount of free water decreases and the resulting decrease in quenching of the excited-state cation results in longer fluorescence lifetimes. Boyd et al.[49] described this kind of quenching in different xanthylium cations. The OG488 dye belongs to this type of cations and thus similar quenching could explain the dependence of k_{0C} on the acid concentration. A modified Stern−Volmer plot describes the quenching process by

$$\frac{1}{\tau_F} = \frac{1}{\tau_F^0} + k_q([H_2O] - [H_2O]^0) \qquad (2)$$

where τ_F is the fluorescence lifetime of C at each acid concentration, and $[H_2O]$ is the amount of "free" water at each acid concentration; $[H_2O]^0$ is the lowest quencher concentration used (corresponding to the highest acidity, 11.1 M), but unlike the standard Stern−Volmer equation this is not exactly zero, although it is close enough; finally, τ_F^0 is the fluorescence lifetime of C at the highest acid concentration. Since the lifetimes are given by $\tau_F = (k_{0C})^{-1}$, and we assumed the water activity (in the molar concentration scale) represents the free water concentration, eq 2 changes into

$$k_{0C} = k_{0C}^0 + k_q(a_{H_2O} - a_{H_2O}^0) \qquad (3)$$

Figure 10 shows the Stern−Volmer plot of the recovered k_{0C} values. As can be seen in the figure, a good linearity was reached ($r^2 = 0.99$), the intercept ($(3.04 \pm 0.05) \times 10^8$ s^{-1}) gave the value of k_{0C} at the lowest quencher concentration (k_{0C}^0), and the slope provided a value of $(3.7 \pm 0.2) \times 10^6$ M^{-1} s^{-1} for the quenching constant k_q. This quenching rate constant value is in the same order of magnitude as those recovered for other xanthylium cations.[49] In addition to this water-induced quenching, we commented in the Results section that perchloric acid concentrations above 8.2 M cause a decrease in steady-state fluorescence intensity. We assign this effect to a quenching due to perchlorate ions at high concentrations. Since the variations in the deactivation rate of the cation with water activity are justified through the "free" water quenching, the quenching due to perchlorate ions would essentially have a static character. Nevertheless, there is a serious experimental problem in studying this quenching, since, at the very high perchloric acid concentrations used, the addition of perchlorate ions results in the precipitation of the salt. Furthermore, the quenching processes in this $[HClO_4]$ range turn out to be quite complex, since this perchlorate-induced quenching could never be separated from the water quenching and studied independently. A similar coexistence of both quenching processes, due to "free" water and perchlorate ions at high $[HClO_4]$, was found in Chromotropic acid by Bardez et al.[16] We assume that a quenching caused by protons, as happens in neutral photoacids such as naphthols, is less likely because of the electrostatic repulsion between positive charges.

We have also performed some experiments varying the temperature. We used a nanosecond instrument and recorded monoexponential decay traces at every emission wavelength since the short decay times are masked by the lamp profile. Thus, these studies attempt to justify the effect of temperature on the cation deactivation rate, reflected in variations in the longest decay time. With the simple measurements performed, we have observed that the deactivation processes increase with temperature. Assuming the rate of radiative decay is essentially not affected by temperature,[67] the decrease of the decay time with temperature would arise from a more effective water quenching. The observed red edge effect implies a relatively structured medium in which an increase in temperature would result in a less organized medium, increasing the amount of "free" water available for quenching or enhanced nonradiative decay, and then, decreasing the cation lifetime.

Finally, the quantification of the rate constant variations described above allows us to calculate the decay times through the usual two-state excited-state equations.[40] In our model, the values for the rate constants are given by $k_{0N} = 3.14 \times 10^8$ s^{-1}, $k_{0C} = [0.304 + 3.7 \times 10^{-3} (a_{H_2O} - a^0_{H_2O})] \times 10^9$ s^{-1}, $k_{NC} = 1.0 \times 10^7 (a_{H_2O})^{2.3}$ s^{-1}, and $k_{CN} \times [H^+]$ the values recovered as $Y - k_{0N}$ (Figure 8). Figure 11 shows both the recovered shortest and longest decay times by means of global analyses and the calculated decay times. The decay times and their tendencies are very well predicted by this proposed model, which takes into account the quenching of the cation due to free water, the dependence of the C deprotonation rate with the amount of water acceptors, and the variation in the reprotonation rate with acid concentration.

Conclusions

In this work, we have extended the study on 2′,7′-difluorofluorescein ESPT reactions, describing the two consecutive ESPT reactions between cationic, neutral, and monoanionic species. We have solved this kinetic system by means of global three-compartmental analysis of a fluorescence decay surface composed of decay traces at pH values between 1.1 and 3.0, and several optical setups. This is one of the few three-compartmental systems solved successfully, and it is the most complex to the best of our knowledge. The cation was found to be a "super" photoacid, showing a very high excited-state deprotonation rate, whereas the ESPT reaction between the neutral and monoanion was found to be controlled by the diffusional reprotonation in this pH range. Although the diffusion-influenced reactions are known to result in nonexponential decay traces, we did not find evidence of this behavior in the decays at this pH range. The exponential approach, and thus the global compartmental analysis, was a valid approximation.

In addition, we have increased the acid concentration up to 11.1 M, and have described some other effects which alter the absorption spectra, the time course of the excited species, and the excited-state processes: (1) The cation absorption spectrum is blue-shifted, up to 7.5 nm, with increasing perchloric acid concentration. We think that this may be due to polarizability effects that affect to the solvent relaxation. (2) The decay traces become multiexponential, even though they can be considered nonexponential traces at the beginning with an exponential contribution at longer times. The shortest decay time tended to increase with increasing acid concentration, which has been attributed to the loss of the "free" water clusters available to act as proton acceptors in the cation excited-state deprotonation, at the extremely high [$HClO_4$]. (3) The longest decay time increased with increasing acid concentration at [H^+] above 5.8 M, as a result of the decrease in physical quenching due to "free" water, similar to that found in other xanthylium cations.

Acknowledgment. A.O. thanks the Spanish Ministry of Education, Culture, and Sports for a Ph.D. fellowship and the travel grants to the I.T.Q.B. (Oeiras) and the K. U. Leuven. He also thanks them for the hospitality during his stays. This work was supported by Grant BQU2002-01311 from the Spanish Ministry of Science and Technology.

Supporting Information Available: Text giving the theory of the global three-compartmental analysis, the program implementation procedure, and details on the fitting of the fluorescence decay surface of OG488 in the pH range 1.1−3.0, including schemes showing the kinetic model and the linking scheme and figures showing the fluorescence decay traces and a linear fitting of the recovered log k'_{CN} vs log([H^+]). This material is available free of charge via the Internet at http://pubs.acs.org.

References and Notes

(1) Haugland, R. P. *Handbook of Fluorescent Probes and Research Products*, 9th ed.; Molecular Probes, Inc.: Eugene, OR, 2002.

(2) Sun, W. C.; Gee, K. R.; Klaubert, D. H.; Haugland, R. P. *J. Org. Chem.* **1997**, *62*, 6469−6475.

(3) Leonhardt, H.; Gordon, L.; Livingston, R. *J. Phys. Chem.* **1971**, *75*, 245−249.

(4) Orte, A.; Crovetto, L.; Talavera, E. M.; Boens, N.; Alvarez-Pez, J. M. *J. Phys. Chem. A* **2005**, *109*, 734−747.

(5) Alvarez-Pez, J. M.; Ballesteros, L.; Talavera, E.; Yguerabide, J. *J. Phys. Chem. A* **2001**, *105*, 6320−6332.

(6) Crovetto, L.; Orte, A.; Talavera, E. M.; Alvarez-Pez, J. M.; Cotlet, M.; Thielemans, J.; De Schryver, F. C.; Boens, N. *J. Phys. Chem. B* **2004**, *108*, 6082−6092.

(7) Orte, A.; Bermejo, R.; Talavera, E. M.; Crovetto, L.; Alvarez-Pez, J. M. *J. Phys. Chem. A.* **2005**, *109*, 2840−2846.

(8) Ameelot, M.; Boens, N.; Andriessen, R.; van den Bergh, V.; De Schryver, F. C. *J. Phys. Chem.* **1991**, *95*, 2041−2047.

(9) Van den Bergh, V.; Boens, N.; De Schryver, F. C.; Ameloot, M.; Gallay, J.; Kowalczyk, A. *Chem. Phys.* **1992**, *166*, 249−258.

(10) Martin, M.; Lindqvist, L. *J. Lumin.* **1975**, *10*, 381−390.

(11) Khalil, M. M. H.; Boens, N.; De Schryver, F. C. *J. Phys. Chem.* **1993**, *97*, 3111−3122.

(12) Hermans, B.; De Schryver, F. C.; Van Stam, J.; Boens, N.; Jerome, R.; Teyssie, P.; Trossaert, G.; Goethals, E.; Schacht, E. *Macromolecules* **1995**, *28*, 3380−3386.

(13) Seixas de Melo, J.; Maçanita, A. L. *Chem. Phys. Lett.* **1993**, *204*, 556−562.

(14) Dias, A.; Varela, A. P.; Miguel, M. da G.; Becker, R. S.; Burrows, H. D.; Maçanita, A. L. *J. Phys. Chem.* **1996**, *100*, 17970−17977.

(15) Reyman, D.; Viñas, M. H.; Poyato, J. M. L.; Pardo, A. *J. Phys. Chem. A* **1997**, *101*, 768−775.

(16) Bardez, E.; Alain, V.; Destandau, E.; Fedorov, A.; Martinho, J. M. G. *J. Phys. Chem. A* **2001**, *105*, 10613−10620.

(17) Drössler, P.; Holzer, W.; Penzkofer, A.; Hegemann, P. *Chem. Phys.* **2002**, *282*, 429−439.

(18) Pant, S.; Tripathi, H. B.; Pant, D. D. *J. Photochem. Photobiol. A: Chem.* **1994**, *81*, 7−11 and references therein.

(19) Shah, J.; Pant, D. D. *Curr. Sci.* **1985**, *54*, 1040−1043.

(20) Pines, E.; Pines, D. In *Ultrafast Hydrogen Bonding Dynamics and Proton-Transfer Processes in the Condensed Phase*; Elsaesser, T., Bakker, J., Eds.; Kluwer Academic Publishers: Dordrecht, The Netherlands, 2003.

(21) Ireland, J. F.; Wiatt, P. A. H. *Adv. Phys. Org. Chem.* **1976**, *12*, 131−221.

(22) Bardez, A.; Chatelain, A.; Larrey, B.; Valeur, B. *J. Phys. Chem.* **1994**, *98*, 2357−2366.

(23) Tolbert, L. M.; Solntsev, K. M. *Acc. Chem. Res.* **2002**, *35*, 19−27.

(24) Pines, E.; Fleming, G. R. *J. Phys. Chem.* **1991**, *95*, 10448−10457.

(25) Rice, S. A. *Diffusion-Limited Reactions; Comprehensive Chemical Kinetics*; Elsevier Biomedical: Amsterdam, 1985; Vol. 25.

(26) Schulman, S. G.; Vogt, B. S. *J. Phys. Chem.* **1981**, *85*, 2074−2079.

(27) (a) Lee, J.; Robinson, G. W.; Webb, S. P.; Philips, L. A.; Clark, J. H. *J. Am. Chem. Soc.* **1986**, *108*, 6538−6542. (b) Robinson, G. W.; Thistlethwaite, P. J.; Lee, J. *J. Phys. Chem.* **1986**, *90*, 4224−4233. (c) Lee, J.; Griffin, R. D.; Robinson, G. W. *J. Chem. Phys.* **1985**, *82*, 4920−4925.

(28) Tolbert, L. M.; Haubrich, J. E. *J. Am. Chem. Soc.* **1994**, *116*, 10593−10600.

(29) (a) Than Htun, M.; Suwaiyan, A.; Klein, U. K. A. *Chem. Phys. Lett.* **1995**, *243*, 71−77. (b) Than Htun, M.; Suwaiyan, A.; Klein, U. K. A. *Chem. Phys. Lett.* **1995**, *243*, 506−511.

(30) Agmon, A.; Huppert, D.; Masad, A.; Pines, E. *J. Phys. Chem.* **1991**, *95*, 10407−10413. Erratum *J. Phys. Chem.* **1992**, *96*, 2020.

(31) Tolbert, L. M.; Harvey, L. C.; Lum, R. C. *J. Phys. Chem.* **1993**, *97*, 13335−13340.

(32) Lee, J. *J. Am. Chem. Soc.* **1989**, *111*, 427−431.

(33) von Smoluchowski, M. *Ann. Phys.* **1915**, *48*, 1103−1112.

(34) Debye, P. *Trans. Electrochem. Soc.* **1942**, *82*, 265−272.

(35) Pines, E.; Huppert, D. *J. Chem. Phys.* **1986**, *84*, 3576−3577.

(36) (a) Pines, E.; Huppert, D.; Agmon, N. *J. Chem. Phys.* **1988**, *88*, 5620−5630. (b) Agmon, N.; Pines, E.; Huppert, D. *J. Chem. Phys.* **1988**, *88*, 5631−5638. (c) Agmon, N. *J. Chem. Phys.* **1988**, *88*, 5639−5642.

(37) Goldberg, S. Y.; Pines, E.; Huppert, D. *Chem. Phys. Lett.* **1992**, *192*, 77−81.

(38) Pines, E.; Magnes, B.-Z.; Lang, M. J.; Fleming, G. R. *Chem. Phys. Lett.* **1997**, *281*, 413−420.

(39) Genosar, L.; Cohen, B.; Huppert, D. *J. Phys. Chem. A* **2000**, *104*, 6689−6698.

(40) Lakowicz, J. R. *Principles of Fluorescence Spectroscopy*; Kluwer Academic/Plenum Publishers: New York, 1999.

(41) Solntsev, K. M.; Huppert, D.; Agmon, N.; Tolbert, L. M. *J. Phys. Chem. A* **2000**, *104*, 4658−4669.

(42) Cohen, B.; Huppert, D.; Agmon, N. *J. Phys. Chem. A* **2001**, *105*, 7165−7173.

(43) Pines, D.; Pines, E. *J. Chem. Phys.* **2001**, *115*, 951−953.

(44) Solntsev, K. M.; Huppert, D.; Agmon, N. *J. Phys. Chem. A* **2001**, *105*, 5868−5976.

(45) Agmon, N.; Szabo, A. *J. Chem. Phys.* **1990**, *92*, 5270−5284.

(46) Rini, M.; Magnes, B. Z.; Pines, E.; Nibbering, E. T. J. *Science* **2003**, *301*, 349−352.

(47) Joshi, H. C.; Gooijer, C.; van der Zwan, G. *J. Phys. Chem. A* **2002**, *106*, 11422−11430.

(48) Wan, P.; Yates, K.; Boyd, M. K. *J. Org. Chem.* **1985**, *50*, 2881−2886.

(49) Boyd, M. K.; Lai, H. Y.; Yates, K. *J. Am. Chem. Soc.* **1991**, *113*, 7294−7300.

(50) Ebbesen, T. W.; Ghiron, C. A. *J. Phys. Chem.* **1989**, *93*, 7139−7143.
(51) Yuan, D.; Brown, R. G. *J. Phys. Chem. A* **1997**, *101*, 3461−3466.
(52) Diehl, H.; Horchak-Morris, N. *Talanta* **1987**, *34*, 739−741.
(53) Maus, M.; Rousseau, E.; Cotlet, M.; Schweitzer, G.; Hofkens, J.; Van der Auweraer, M.; De Schryver, F. C. *Rev. Sci. Instrum.* **2001**, *72*, 36−40.
(54) Demchenko, A. P. *Luminescence* **2002**, *17*, 19−42.
(55) Yu, H.; Kwon, H. J.; Jang, D. J. *Bull. Korean Chem. Soc.* **1997**, *18*, 156−161.
(56) Watkins, A. R. *J. Chem. Soc., Faraday Trans. 1* **1972**, *68*, 28−36.
(57) Barrash-Shiftan, N.; Brauer, B. B.; Pines, E. *J. Phys. Org. Chem.* **1998**, *11*, 743−750.
(58) Lima, J. C.; Abreu, I.; Brouillard, R.; Maçanita, A. L. *Chem. Phys. Lett.* **1998**, *298*, 189−195.
(59) Moreira, P. F.; Giestas, L.; Yihwa, C.; Vautier-Giongo, C.; Quina, F.; Maçanita, A. L.; Lima, J. C. *J. Phys. Chem. A* **2003**, *107*, 4203−4210.
(60) Kim, T. G.; Topp, M. R. *J. Phys. Chem. A* **2004**, *108*, 10060−10065.
(61) Solntsev, K. M.; Agmon, N. *Chem. Phys. Lett.* **2000**, *320*, 262−268.
(62) Conte, J. C.; Martinho, J. M. G. *Chem. Phys. Lett.* **1987**, *134*, 350−354.
(63) Huppert, D.; Kolodney, E.; Gutman, M.; Nachliel, E. *J. Am. Chem. Soc.* **1982**, *104*, 6949−6953.
(64) Schulman, S. G.; Kelly, R. N.; Gonzalez, J. *Pure Appl. Chem.* **1987**, *59*, 655−662.
(65) Shizuka, H.; Ogiwara, T.; Narita, A.; Sumitani, M.; Yoshihara, K. *J. Phys. Chem.* **1986**, *90*, 6708−6714.
(66) Isaacs, N. *Physical Organic Chemistry*, 2nd ed.; Addison-Wesley Longman: Harlow, U.K., 1995.
(67) Ware, W. R.; Baldwin, B. A. *J. Chem. Phys.* **1965**, *43*, 1194−1197.